

Article

A Comparative Kinetic Study of Pb and Pb-Sb Electrodes in Sulfuric Acid Solutions

E.N. Codaro, and F.E. Varela*

Instituto de Investigaciones Fisicoquímicas Teóricas y Aplicadas (INIFTA), Fac. de Cs.Ex. (U.N.L.P.), Sucursal 4 - C.C. 16, (1900) La Plata, Argentina

Received: June 30, 1996; January 20, 1997

As respostas eletroquímicas de eletrodos de Pb e de Pbs-3.4%Sb em H₂SO₄ 5 M foram examinadas combinando as técnicas de varredura e saltos de potencial. A presença do antimônio evita o bloqueio completo da superfície ativa do eletrodo por cristais de PbSO₄ durante a eletrooxidação, mudando a composição e a estrutura da camada passiva. A eletrooxidação do Sb tem sido interpretada em termos de um mecanismo de adsorção-dissolução onde um elétron é transferido na etapa determinante da velocidade. A cinética de crescimento da camada interna de PbO também tem sido estudada. No eletrodo de Pb-Sb, a velocidade de crescimento do PbO diminui devido a uma mudança no mecanismo de transporte dos íons através da camada anódica.

The electrochemical responses of Pb and Pb-3.4% Sb electrodes in 5 M H₂SO₄ were examined combining potential sweep and potential step techniques. The presence of antimony prevents the complete blockage of the electrode active surface by PbSO₄ crystals during electro-oxidation, changing the composition and structure of the passive layer. The electro-oxidation of Sb was interpreted in terms of an adsorption-dissolution mechanism where in the rate-determining step one electron is transferred. The growth kinetics of the PbO inner layer was also studied. On the Pb-Sb electrode, the growth rate of PbO decreases because of a change in the transport mechanism of ions through the anodic layer.

Keywords: *lead-antimony/sulfuric acid system, lead-antimony electro-oxidation, lead-antimony alloy electrochemical behavior*

Introduction

In a lead-acid battery, the performance of positive plates depends on the grid corrosion processes and the softening and shedding of PbO₂ electrode active material¹. Antimony is widely used as a grid alloying element for this kind of battery. However, the exact influence of Sb on the chemical nature of the reaction products and on the morphology of the positive electrode active material is still open to discussion.

There is general agreement on some stages involved in the overall reaction of Pb and Pb-Sb electrodes in sulfuric acid electrolytes. During anodic polarization, the reaction between Pb²⁺ and SO₄²⁻ ions occurs, and a semi-permeable PbSO₄ crystal layer is formed. In order to maintain electroneutrality, the solution in the pores is alkalized as a result of water dissociation and the migration of H⁺ ions from the

inner layer to the bulk solution, whereby a pH gradient appears. At anodic potentials higher than 0.23 V vs. NHE, the electro-oxidation of Sb and the formation of tet-PbO begin, and several chemical reactions take place, resulting in the formation of substituted lead antimony oxides and SbO⁺ ions². Thus, the anodic layer is composed of PbSO₄ and an inner film involving basic Pb(II)- and Sb(III)-containing compounds (like basic sulfates, hydroxides and oxides) which builds up progressively beneath the initial PbSO₄ porous layer structure³.

The purpose of the present research is to study the electrochemical behavior of Pb and Pb-Sb electrodes in 5 M H₂SO₄ under controlled conditions in order to quantitatively evaluate the present phases in the anodic layer.

Experimental

The experimental setup has been described in previous publications^{4,5}. "Specpure" lead and lead-antimony (3.4 wt% Sb) alloy disks (Johnson Matthey Chemicals, 0.30 cm² apparent area) embedded in PTFE holders were used as the working electrodes in 5 M H₂SO₄ at 25 °C, under purified nitrogen gas saturation. The electrodes were mechanically polished with 600 and 1200 grade emery papers and thoroughly rinsed in four fold distilled water. Potentials were measured and referred to in the text, against a Hg/Hg₂SO₄, K₂SO₄ (sat.) reference electrode.

Prior to the electrochemical runs, working electrodes were cathodized for 5 min at -1.30 V, *i.e.* in the hydrogen evolution reaction (HER) potential range, to achieve a reproducible electroreduced electrode surface. Subsequently, two types of experiments were made: *i*) characteristic current density/potential (j/E) curves under different hydrodynamic conditions were recorded by applying either single (STPS) or repetitive (RTPS) triangular potential sweeps between preset cathodic ($E_{s,c} = -1.30$ V) and anodic ($E_{s,a}$) switching potentials at scan rate v , including a potential holding at $E_{s,a}$ for different times τ ; *ii*) combined linear potential scans with potential steps were used to study the electro-oxidation process of antimony during the forward potential sweep.

Results and Discussion

The voltammogram of Pb in 5 M H₂SO₄ solution at $v = 0.04$ V s⁻¹ run between $E_{s,c} = -1.30$ V and $E_{s,a} = 1.40$ V (Fig. 1) shows an anodic current peak (A1) at *ca.* -0.96 V followed by a wide passive region during the forward potential sweep⁶. During the reverse scan, two cathodic

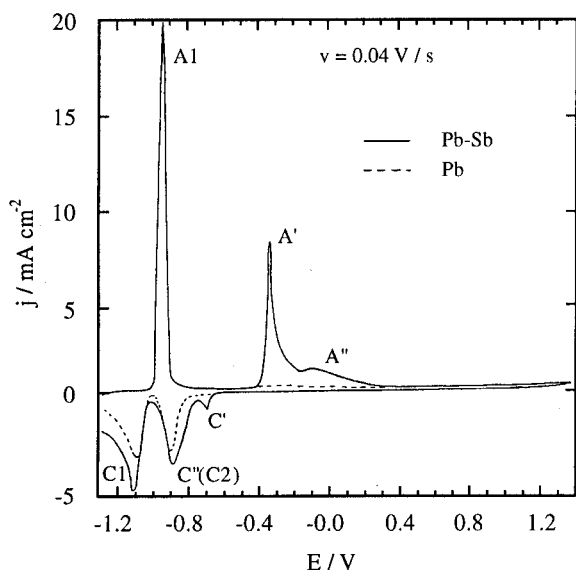


Figure 1. Comparative voltammograms of Pb (full curve) and Pb-Sb (dashed curve) electrodes in 5 M H₂SO₄ solution run at $v = 0.040$ V s⁻¹ between $E_{s,c} = -1.30$ V and $E_{s,a} = 1.40$ V.

current peaks, C1 and C2, are observed at -1.11 V and -0.95 V, respectively. Conjugated current peaks A1 and C1 correspond to the electro-oxidation of Pb to PbSO₄ and to the electroreduction of PbSO₄^{7,8}, whereas peak C2 may be associated with the electroreduction of PbO which builds up progressively beneath the initial PbSO₄ porous layer⁹. Electrochemical measurements performed using the Pb-3.4%Sb electrode (Fig. 1) reveal additional current contributions: two anodic current peaks at -0.37 and -0.15 V (A' and A'') located in the region of stable Pb(II) surface compounds, and two cathodic peaks (C' and C'') at -0.69 and -0.86 V preceding the PbSO₄ electroreduction potential range. Current peaks A' and C' may be related to the electroformation and electroreduction of the Sb(III) species, whereas the broad peaks A'' and C'' seem to be associated with the formation of Sb(III) complexes and the complex electroreduction of basic Pb(II)-Sb(III) containing surface compounds (C2-C''), respectively. The whole potentiodynamic response is practically independent of the solution stirring conditions.

The analysis of peak parameters during consecutive potentiodynamic charge/discharge cycles between

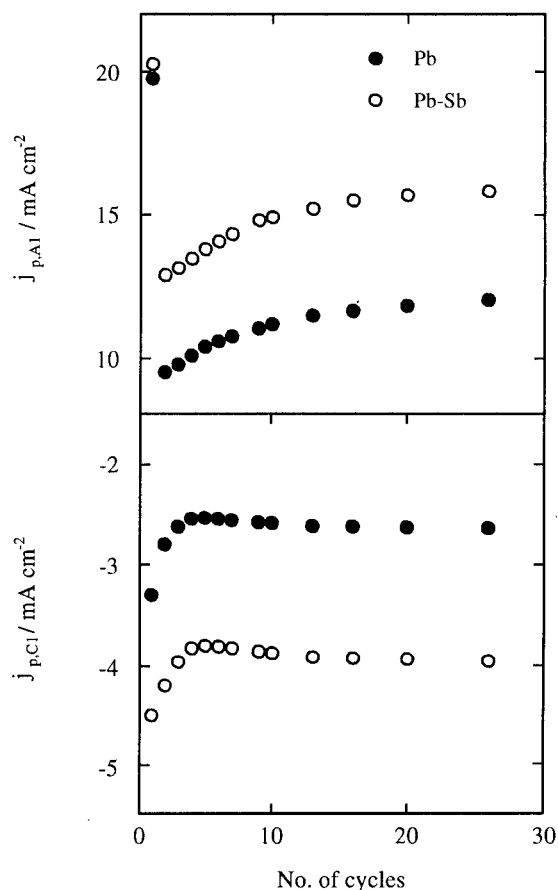


Figure 2. The dependences of $j_{p,A1}$ and $j_{p,C1}$ on the number of cycles for Pb and Pb-Sb electrodes. Data obtained from cyclic voltammograms run between $E_{s,c} = -1.30$ V and $E_{s,a} = 1.40$ V at $v = 0.040$ V s⁻¹.

$E_{s,c} = -1.30$ V and $E_{s,a} = 1.40$ V at $v = 0.04$ V s⁻¹ on both Pb and Pb-Sb electrodes, reveals gradual structural changes of the passivating layer (Fig. 2). The height of conjugated current peaks A1 and C1 decreases abruptly in the initial cycles, reaches a minimum current value, and then increases slowly to attain a stabilized response after about twenty cycles. Moreover, the peak potentials $E_{p,A1}$ and $E_{p,C1}$ remain practically constant during cycling. On the other hand, peak C2 gradually tends towards more negative potentials and its charge density (q_{C2}) decreases to approach the stationary value after prolonged cycling (Fig. 3). The voltammetric charge involved in current peaks A1, C1, and C2 for measurements performed using Pb electrodes is smaller than that recorded employing Pb-Sb electrodes (Figs. 2 and 3b). The dissolution of the Sb(III) species increases the permeability of the passive layer. The Pb ions can then diffuse more easily through the anodic film and the pH inside the passive layer decreases. This explains the fact that the charge and reduction overpotentials of basic Pb(II) compounds decrease more quickly for alloy electrodes during cycling.

The height of current peaks A' and C', which are obtained with Pb-Sb electrodes and are related to the electroformation/electroreduction of Sb(III)-containing surface species, gradually diminishes during cycling to attain stable values at about twenty cycles (Fig. 4). The charge density ratio of peaks A' and C' is practically constant ($q_{A'}/q_{C'} \approx 4$) with both the number of cycles and potential scan rate, at least up to the 50th potential cycle and for v

values within the 0.02 V s⁻¹ $\leq v \leq 0.20$ V s⁻¹ range, respectively. The same electrochemical behavior for $E_{s,a} = 0.00$ V was also observed. This suggests that the formation and reduction processes of Sb(III)-containing species take place at preferential surface sites limited to the areas unblocked by residual lead sulfate, which seems to be highly resistant to prolonged electroreduction^{10,11}. Moreover, these results imply that only the ions nearest to the electrode surface can be electroreduced, *i.e.* those associated with the adsorption mechanism. Therefore, for high cycle number, the dissolution process appears to be inhibited by chemisorption of $[\text{Sb}(\text{SO}_4)_2]^-$ or $[\text{SbOSO}_4]^-$ anions. On the other hand, the change of $j_{p,A'}$ and $j_{p,C'}$ during initial potential cycles may be associated with the gradual formation of a more regular structure of the surface layer (*i.e.* a more homogeneous size of the PbSO_4 crystals) and, accordingly, the decrease of voltammetric charge density of peaks A', C' and C2 can be related to processes which contribute to enhance surface layer porosity. These conclusions agree with scanning electron microscopy (SEM) results obtained on Pb and Pb-Sb electrodes under similar experimental conditions by Bialacki *et al.*¹² and Webster *et al.*¹³. Webster *et al.* concluded from their observations that antimony alloy electrodes have surface films of higher porosity and that the porosity increases with cycling.

The electro-oxidation of Sb to the Sb(III) species at potentials between -0.50 V and 0.00 V was studied by potential sweep and potential step combining measurements. Figs. 5a and 5b present the dependence of $E_{p,A'}$ on $\log v_a$ and $j_{p,A'}$ on $v_a^{1/2}$ after $\tau = 1$ min at $E_{s,a} = -0.50$ V. These linear relationships are typical of an irreversible system. This is consistent with the fact that $j_{p,A'} \gg j_{p,C'}$ for the whole scan rate range. Also, these relationships may be associated with an EC reaction where the electron transfer

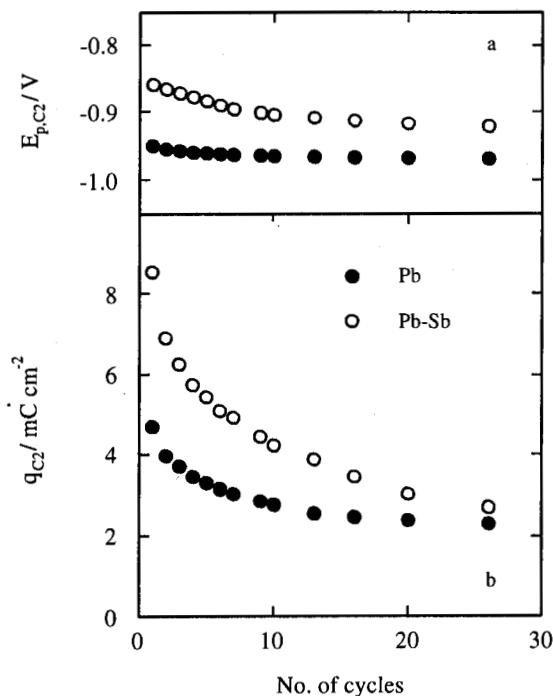


Figure 3. The dependences of (a) $E_{p,C2}$ and (b) q_{C2} on the number of cycles in both electrode systems, under the same conditions as in Fig 2.

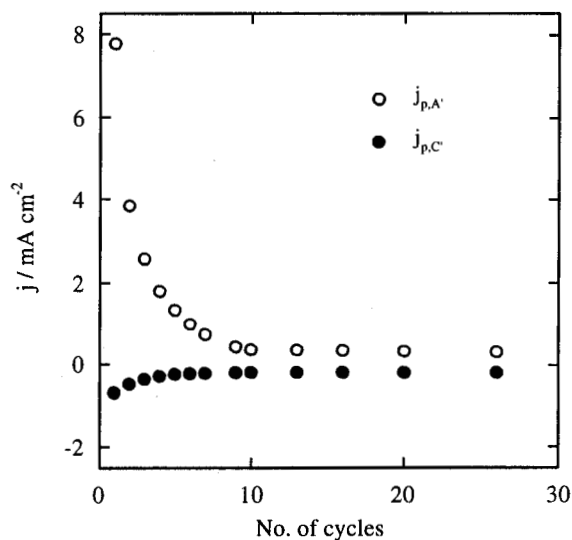


Figure 4. The dependences of $j_{p,A'}$ and $j_{p,C'}$ on the number of cycles for Pb-Sb electrodes, under the same conditions as in Fig 2.

is reversible and the chemical reaction is irreversible¹⁴. Thus, $E_{p,A'}$ varies with the sweep rate as shown by the theoretical equation:

$$E_p = K - \frac{2.303RT}{2\alpha n_\alpha F} \log v_a \quad (1)$$

where K is independent of v_a . The experimental slope value is $(\partial E_{p,A'}/\partial \log v_a) = 0.0495$. Thus, the calculated value of αn_α is 0.6, where n_α , the number of electrons involved in the rate-determining step, can be assumed to be 1.

Taking into account the above considerations, the electro-oxidation of Sb can be interpreted as two consecutive electronic transfer steps and one chemical reaction, which corresponds to the fast dissolution of an electro-oxidation product. Accordingly, the electroreduction charge during the negative potential sweep is smaller than that developed in the electro-oxidation process.

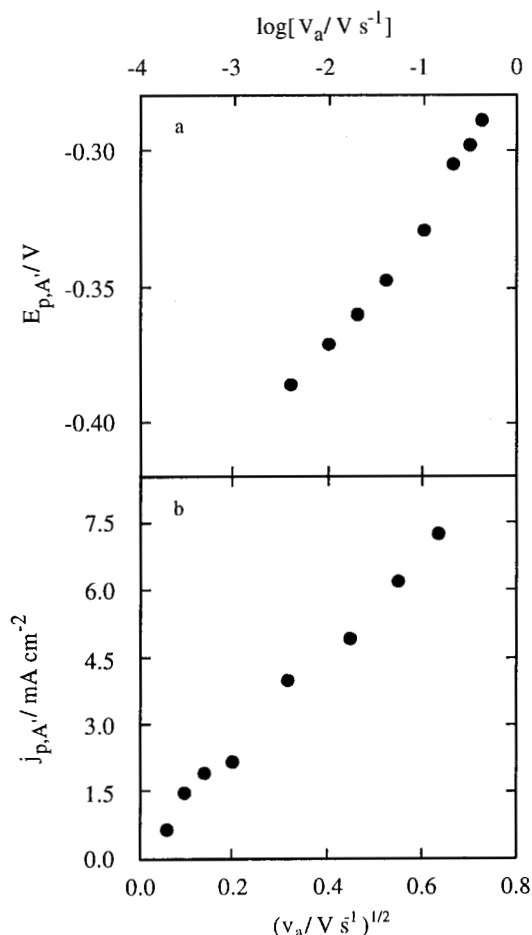
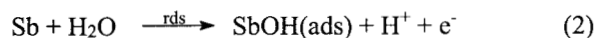
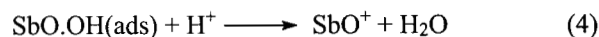
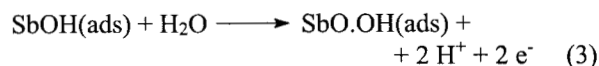


Figure 5. The dependences of (a) $E_{p,A'}$ and (b) $j_{p,A'}$ on v_a . Data obtained from voltammograms recorded in the potential region of peaks A' and A'', after $\tau = 1$ min at $E_{s,a} = -0.50$ V.



The pH decrease resulting from steps (2) and (3) contributes to the dissolution of the anodic layer basic compounds, oxides and hydroxides of Sb(III), as well as those of Pb(II).

To investigate the electroformation of PbSO_4 and PbO layers, the Pb and Pb-Sb electrodes were anodized at several $E_{s,a}$ in the passive potential range for different polarization times (τ). From the analysis of electroreduction peak C1, it was found that the amount of PbSO_4 formed on Pb electrodes is almost independent of potential and increases slightly with τ (Fig. 6a,b), in agreement with reported data¹⁵. On Pb-Sb electrodes, on the other hand, the peak C1 charge depends on $E_{s,a}$, and is higher than that obtained on Pb electrodes.

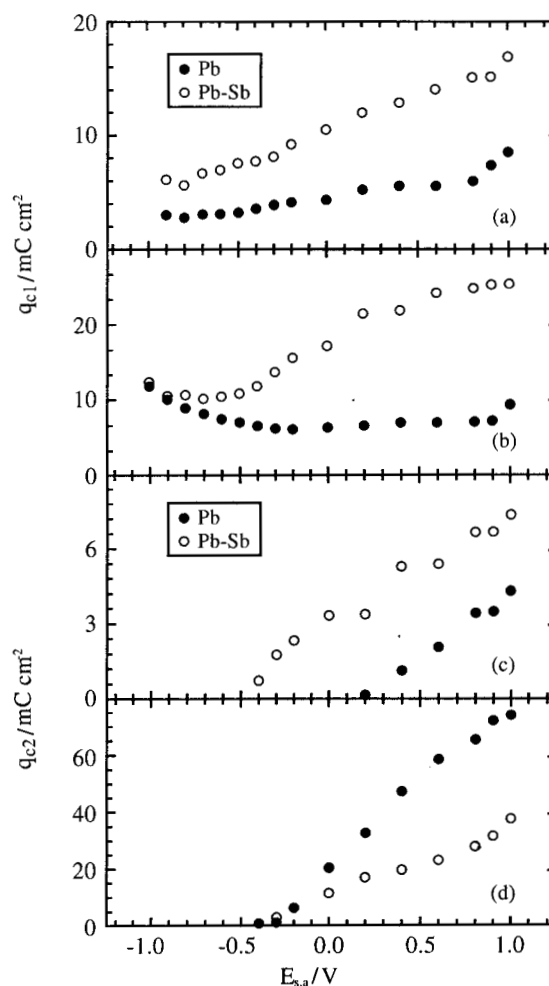


Figure 6. The dependences of q_{C1} and q_{C2} on $E_{s,a}$ for different anodic polarization times: (a) and (c) $\tau = 0$ min, (b) and (d) $\tau = 60$ min. $E_{s,c} = -1.30$ V; $v = 0.020$ V s⁻¹.

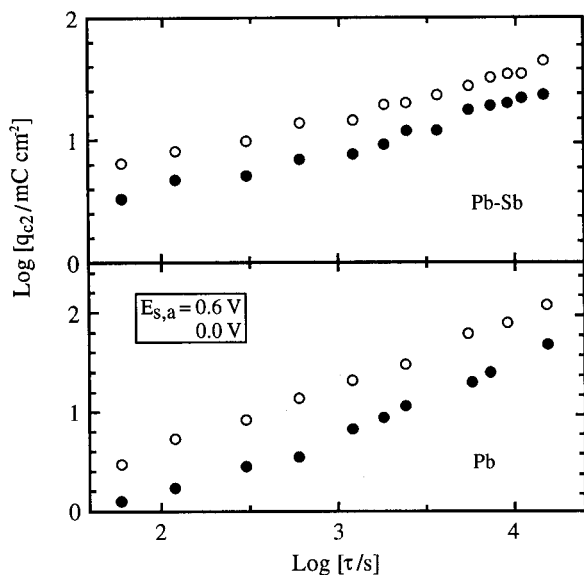


Figure 7. The dependences of qc_2 on τ for different $E_{s,a}$, $E_{s,c} = -1.30$ V; $v = 0.020$ V s⁻¹.

Figs. 6c and 6d show that the PbO electroreduction charge increases linearly with the potential, but the relative amounts for Pb and Pb-Sb electrodes shown an inversion with τ . This can be explained by a dissolution of the small crystals of basic Sb(III) compounds during anodization.

From the $\log qc_2$ vs. $\log \tau$ plot (Fig. 7), linear relationships for each $E_{s,a}$ in the 0.0 to 0.6 V potential range are obtained. Higher PbO growth rates on Pb than those on Pb-Sb are obtained, and the ratio between both PbO charge densities, that obtained on Pb and that on Pb-Sb, gives results proportional to $\tau^{1/3}$. As the charge density qc is practically independent of $E_{s,a}$ and τ , these results imply that the dissolution process of Sb(III)-containing species within the pores modified the transport mechanism of the ions (*i.e.* H⁺, OH⁻) through the anodic layer and the growth kinetics of the PbO inner film.

Conclusions

Voltammetric results obtained on Pb-Sb alloy electrodes show that the order within the anodic layer structure increases with potentiodynamic cycling, and the electro-oxidation/electroreduction of Sb species occurs at preferential sites on the surface. The electrooxidation of Sb may

be associated with an adsorption-dissolution mechanism where one electron is transferred in the rate-determining step. The growth rate of the PbO inner film on Pb-Sb electrodes is smaller than that on Pb electrodes, due to a change in the transport mechanism of ions (OH⁻ or H⁺) through the anodic layer.

Acknowledgments

This research project was financially supported by the Consejo Nacional de Investigaciones Científicas y Técnicas and the Comisión de Investigaciones Científicas de la Provincia de Buenos Aires.

References

1. *Advances in Lead-Acid Batteries*; Bullock, K.R.; Pavlov, D., Eds.; The Electrochemical Society, N.J., 1984.
2. Laihonen, S.; Laitinen, T.; Sundholm, G.; Yli-Pentti, A. *Electrochim. Acta* **1990**, *35*, 229.
3. Pavlov, D.; Monahov, B.; Sundholm, G.; Laitinen, T. *J. Electroanal. Chem.* **1991**, *305*, 57.
4. Varela, F.E.; Codaro, E.N.; Vilche, J.R. *J. Braz. Chem. Soc.* **1994**, *5*, 145.
5. Varela, F.E.; Gassa, L.; Vilche, J.R. *J. Appl. Electrochem.* **1995**, *25*, 358.
6. Varela, F.E.; Gassa, L.; Vilche, J.R. *J. Electroanal. Chem.* **1993**, *353*, 147.
7. Varela, F.E.; Vela, M.E.; Vilche, J.R.; Arvia, A.J. *Electrochim. Acta* **1993**, *38*, 1513.
8. Varela, F.E.; Vilche, J.R.; Arvia, A.J. *Electrochim. Acta* **1994**, *39*, 401.
9. Varela, F.E.; Codaro, E.N.; Vilche, J.R. *Electrochim. Acta* **1995**, *40*, 1183.
10. Guo, Y.; Chen, J. *J. Electrochem. Soc.* **1992**, *139*, L99.
11. Trettenhahn, G.L.; Nauer, G.E.; Neckel, A. *Ber. Bunsenges. Phys. Chem.* **1993**, *97*, 422.
12. Bialacki, J.A.; Hampson, N.A.; Peters, K.; Williams, A.K. *J. Appl. Electrochem.* **1983**, *13*, 103.
13. Webster, S.; Mitchell, P.J.; Hampson, N.A.; Dyson, J.I. *J. Electrochem. Soc.* **1986**, *133*, 133.
14. Greef, R.; Peat, R.; Pletcher, D. In *Instrumental Methods in Electro-chemistry*; John Wiley & Sons; N.Y., 1985, Chap. 6.
15. Guo, Y. *J. Electrochem. Soc.* **1995**, *142*, 3378.